Received 20 January 2022
Revised 12 July 2022
13 September 2022
Accepted 9 October 2022

An algorithm for determining the inner and outer loops of arbitrary parametric surfaces

Chuanming Ju
Yantai University, Yantai, China
J. Zhang
Hunan University, Changsha, China
Yong Zhang
PLA Navy Submarine Academy, Qingdao, China, and
Xianfeng Du, Zheng Yuan and Tangying Liu
Yantai University, Yantai, China

Abstract

Purpose – The purpose of this paper is to present an algorithm for determining the inner and outer loops of arbitrary parametric surfaces.

Design/methodology/approach – The algorithm considers two sub-algorithms: one for non-closed surfaces and another one for closed surfaces. The first sub-algorithm named by area positive and negative method (APNM), combines a curve discretization algorithm with the polygon direction judgment algorithm to judge the inner and outer loops of non-closed surfaces. The second sub-algorithm, called by cross-period number method (CPNM), combines a curve discretization algorithm with the periodicity of closed surfaces to judge the type of boundary loops.

Findings – The APNM can use less CPU time to determining the inner and outer loops of the non-closed parametric surfaces. The CPNM can also determine the inner and outer loops of closed parametric surfaces effectively. The judgment results of loops can ensure that the direction of meshes generated on these surfaces is right. And finally ensure the correctness of the numerical simulation results.

Originality/value – Several numerical examples presented have verified the robustness and efficiency of the proposed algorithm. Compared with the conventional algorithm, the more complex the model, the more time the APNM saves in the process of determining the inner and outer loops for non-closed surfaces. The CPNM is also a new method to determining the inner and outer loops for closed parametric surfaces. The single run-time of CPNM is very small and can reach the level of microseconds.

Keywords Inner and outer loops, Parametric surface, Curve discretization, Mesh generation

Paper type Research paper

1. Introduction

The geometric and topological information of geometric model in 3D modeling software are often represented by boundary representation (B-rep) (Thompson *et al.*, 1999; Hoffmann, 1989; Guan *et al.*, 2003a). In the B-rep, the boundary of geometric models consists of several adjacent surfaces, and the boundary of a surface is composed of one or more closed loops. The closed loops can be classified into two types, inner loop and outer loop. The judgment of the loop-type is the basis for determining the side of a region (Shi and Xiao, 1997).

When meshing a surface of geometric model, it is necessary to determine the types of all loops on the surface, and then the orientations of the elements obtained by mesh generation methods are defined (Zheng and Chen, 2016; George, 1996; Lo, 2015; Shewchuk, 2014). The method for judging inner and outer loops has been mentioned in literature (Zheng and Chen, 2016).

This work was supported by National Natural Science Foundation of China under grant numbers 11772125 and 11972010.

Engineering Computations
Vol. 40 No. 1, 2023
pp. 296-310

0264-4401
DOI 10.1108/EC-01-2022-0036

The outer loop is the largest loop on the plane, and other loops are inner loops. However, this method is limited to judging the type of loops on the plane. In addition, a method in anther reference (Shi and Xiao, 1997) is suitable for closed boundary loops composed of straight lines and arcs. However, for engineering structures, curved surfaces are common, such as aircraft skin, vehicle shell, spherical tank, condensing tower, etc. These surfaces are composed of regular curved surfaces and free-form surfaces, such as cylinder, cone, sphere or Bezier (Guan *et al.*, 2003b; Nasri, 1987; Chen *et al.*, 2015; Ameddah and Assas, 2011). Therefore, it is important to judge the inner and outer loops for curved surfaces.

In this paper, an improved algorithm is proposed to determine the inner and outer loops for an arbitrary parametric surface. According to whether the surface is closed or not, this algorithm performs two sub-algorithms, namely area positive and negative method (APNM) and cross-period number method (CPNM) respectively. For non-closed surface (non-periodic surface and non-closed periodic surface), the APNM is employed. In the APNM, the boundary loops of surfaces are discretized by a curve discretization algorithm, so that the closed polygon can be obtained in the parametric plane of the surface. This method only needs to discrete the loop into a few segments and judge whether the corresponding loop is an inner or outer loop by the positive and negative areas of the polygon in the parameter plane, thus reducing the calculation amount. For a closed periodic surface, the CPNM is applied to determine the inner and outer loops of the periodic surface by calculating the number of times by which the loop crosses the periodic line. The algorithm process is shown in below Figure 1.

This paper is organized as follows. Section 2 and Section 3 give the details of APNM and CPNM respectively. In Section 4, results are given to illustrate the effectiveness of APNM and CPNM. The paper ends with conclusions in Section 5.

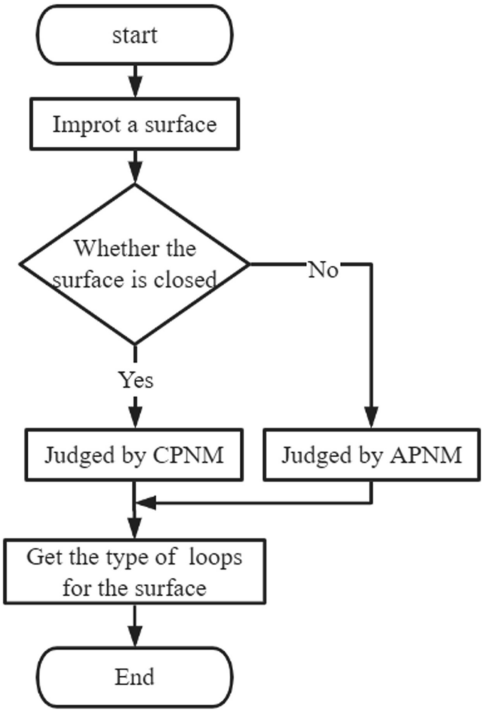

Figure 1.
Flow diagram of the proposed algorithm

2. The detail of APNM

In the section, the detail of APNM is introduced. The APNM employs a curve discrete algorithm to discrete one loop on a curved surface and get a closed polygon in the parametric plane of this surface. The APNM transforms the judgment from the loop on 3D curved surface to the polygon on 2D plane. And then the type of loop is determined by judging the direction of the polygon.

For the boundary loops of a non-closed surface, the region enclosed by them in the parameter plane is single connected or multi-connected domain. The non-closed surface has only one outer loop, and the outer loop is the outermost loop of the surface. Thus, the outer loop must own the largest area in parametric plane compared with other loops (Zheng and Chen, 2016). However, it is very difficult to calculate the real area of a loop in the parameter plane, so we propose a curve discretization method namely dichotomous method (see Section 2.1). The dichotomous method can discretize a boundary loop based on its curvature. After the boundary loop is discretized, the boundary loop can be approximated by several segments, which are mapped into a closed planar polygon in the parametric plane. Then the area size method (ASM) (Zheng and Chen, 2016) is used, and the inner and outer loops are determined by comparing the areas of polygons corresponding to all loops. The largest one is the outer loop, and the rest are the inner loops (see Section 2.2 for the calculation of the area). However, judging the loop-type according to the area requires a lot of calculations. This is because the loop is discretized by many segments, so that the polygon can approximate the loop in parameter space. Therefore, we further propose the APNM. In the APNM, the type of loops is judged by the orientation of the polygon in the parameter plane (see Section 2.3).

2.1 Dichotomy method for curve discretization

The main idea of dichotomy method is to discretize a boundary curve of a surface in two parts continuously until a given subdivision condition is not satisfied, and then the subdivision procession is stopped. The given subdivision condition will determine the final number of discrete segments of the curve. The process is shown in Figure 2.

Arc *ab* is a curve, equation (1) is employed to evaluate the degree of curvature of the arc. If *R* is larger, it means that the curvature of the arc is greater, and the string *ab* cannot approximate the arc *ab*. If *R* is larger than a given ratio, the arc *ab* is divided into arc *ac* and arc *bc*, this process continues recursively until the *R* of all arcs is less than the given curvature ratio.

$$R = \frac{l_{\overset{\frown}{AB}} - l_{\overline{AB}}}{l_{\overset{\frown}{AB}}} \tag{1}$$

This method is simple and stable and can adjust the given curvature ratio to get different discretization results, as shown in Figure 3.

2.2 Calculation of polygon area

According to Green's formula, the area formula of polygon (Li *et al.*, 2011) can be obtained, and the area value of polygon is calculated by curve integral of coordinates. Green's formula is as follows:

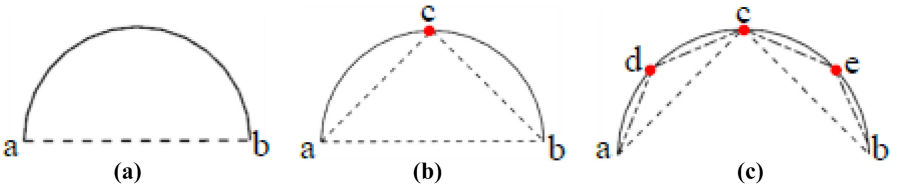

Figure 2.
Process of dichotomous method: (a) initial curve; (b) discretize results for once; (c) discretize results for twice

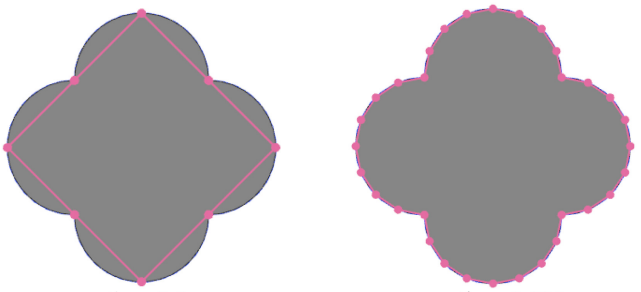

Figure 3.
Discretized results of curve according to different ratios

$$\iint_D \left(\frac{\partial Q}{\partial x} - \frac{\partial P}{\partial y}\right) dxdy = \oint_L Pdx + Qdy \tag{2}$$

where L is the positive boundary curve of region D, and the positive boundary curve L is defined as the left side of region D when the observer walks along the boundary curve.

From Green's formula (2), the area formula of polygonal region D is obtained:

$$S_D = \iint_D 1dxdy. \tag{3}$$

When $p = 0, Q = x$, Green's formula (3) is changed to:

$$\iint_D 1dxdy = \oint_L xdy = \sum_{i=1}^{N} \oint_{Li} xdy \tag{4}$$

The area of polygon S_D is transformed from area integral to line integral, where the boundary curve L is composed of closed line segments, such as $L_1, L_2 \cdots L_N$.

Because the coordinates of two ends of the line segments are known, the equation of the line segments can be obtained according to the two-point formula of the linear equation. The equation for line segment L_i is shown in the follows:

$$\begin{aligned} &L_i : \left(y - y_i^0\right)\left(x_i^1 - x_i^0\right) = \left(x - x_i^0\right)\left(y_i^1 - y_i^0\right), \\ &x_i^0 < x < x_i^1, y_i^0 < y < y_i^1, \end{aligned} \tag{5}$$

where $(x_i^0, y_i^0), (x_i^1, y_i^1)$ are the coordinates of two end points of each line segment. Taking formula (5) into formula (4), we get the following results:

$$S_D = \sum_{i=1}^{N} \int_{L_i} (-\mathrm{y}) dx = \frac{1}{2} \sum_{i=1}^{N} \left(x_i^0 + x_i^1\right)\left(y_i^1 - y_i^0\right), \tag{6}$$

where $(x_i^0, y_i^0), (x_i^1, y_i^1)$ are the coordinates of two end points of the line segment L_i $(i = 1, 2, 3 \cdots N)$.

2.3 Area positive and negative method (APNM)

If the type of a loop is judged by the ASM, the amount of calculation is relatively large. This is because that the loop is discrete into many segments, so that the polygon can approximate the

loop in the parameter space. In order to reduce the amount of calculation, we propose the APNM to judge the type of loop. In 3D modeling software, the boundary representation method (B-rep) is employed to express the 3D geometric model. For boundary loops of a surface, their directions are defined as the surface is located in the left region of loop along the direction of the loop. In the B-rep, if the normal vector of the surface and that of its parametric plane point to the same direction, the direction of the outer loop on the parametric plane of the surface is counterclockwise, and the direction of the inner loop on the parametric plane of the surface is clockwise. If the normal vector of the surface and that of the parameter plane point in opposite directions, then the direction of the outer loop on the parameter plane of the surface is clockwise, and the direction of the inner loop in the parameter plane of the surface is counterclockwise. According to this characteristic, we use the dichotomy method to discretize the loop and then get the corresponding polygon in the parameter plane. The type of loop is determined by judging the direction of the polygon.

The direction judgment of polygon is a basic algorithm about polygon (Feito *et al.*, 1995; Feito and Torres, 1997), which is not only widely used in computer graphics, moreover, there are many applications in visualization of scientific computing which is a popular research field of computer science (Ke, 2005; Zlatko, 1998; Wolfe, 2002; Tate and Jared, 2003). In this paper, the direction of polygon is determined by calculating the positive and negative integral value of area. This method firstly discretizes loop to get the polygon according to the dichotomy method. It should be noted that the given curvature in the dichotomy method does not need to be set very small. This is because that the discrete polygon in the parameter plane does not need to approximate the loop, but the direction of the obtained polygon needs to be consistent with the direction of the loop in parameter space, which can be naturally obtained in the dichotomy method.

Secondly, according to whether the normal vector of the surface and that of the parameter plan are consistent, we can judge whether the direction of the polygon needs to be adjusted to the opposite direction. If they are consistent, the direction of the polygon needs not to change. If they are not consistent, we need to adjust the direction of the polygon. The purpose of adjusting the direction of the polygon is to unify the judgment criteria. The counterclockwise polygon is an outer loop, and the clockwise polygon is an inner loop.

Finally, the area of the polygon is calculated by Green's formula. If the integral value of the polygon area is positive, the direction of the polygon is counterclockwise, the according loop is the outer loop; On the contrary, if the area of polygon is negative, the direction is clockwise, the according loop is an inner loop. The advantage of this method is that it only needs to discretize the loop into a polygon with a few segments in the parameter space, and the amount of calculation is obviously less than the ASM. The flow chat of the APNM is shown in Figure 4.

3. The detail of the CPNM

A non-closed periodic surface can obtain single connected or multi-connected regions in its parameter plane, so its area in the parameter plane can be approximately calculated to determine the loop-type of this surface. However, the boundary information of a closed periodic surface is missing in its parameter plane (Du *et al.*, 2007). That is to say, after the boundary loop of a closed periodic surface is discretized, a closed polygon cannot be formed in the parameter plane of the surface, so the APNM is invalid for the closed periodic surface.

In order to solve the above problems, according to the periodicity of closed periodic surfaces, the cross-period number method (CPNM) is proposed in this paper to judge the inner and outer loops for closed periodic surfaces. The detail process of CPNM is illustrated in Figure 5. First of all, we need to discretize the boundary loop of a closed surface with dichotomy method. It is worth noting that it is not necessary to discretize many segments to

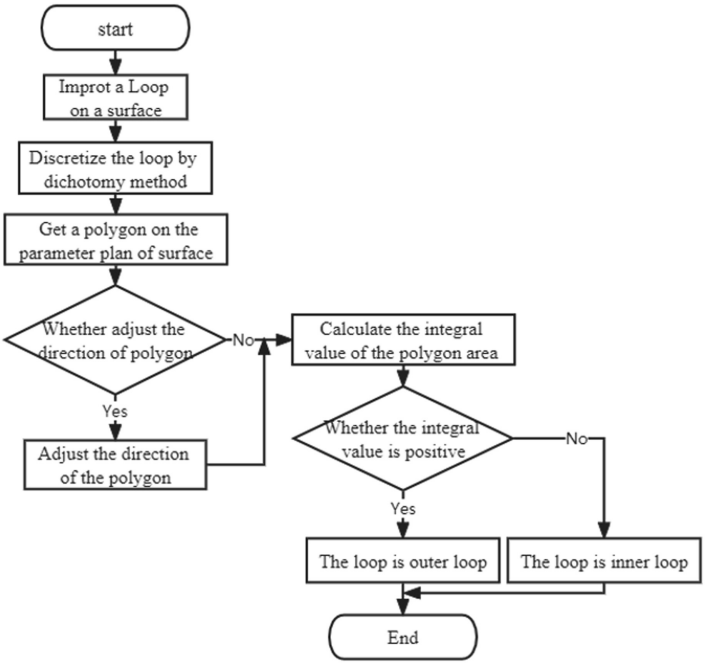

Figure 4.
Flow diagram of the APNM

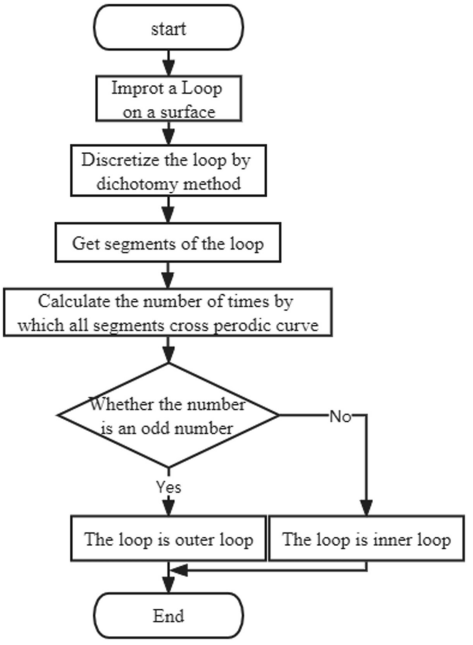

Figure 5.
Flow diagram of the CPNM

approximate the loop. The given ratio does not need to be set very small. Ensure the parameter coordinates of every two transformed points do not exceed a half of one period, a loop is generally subdivided into more than four segments. Then judge whether the parameter coordinates of each two discrete points are cross-period and calculate the total cross-period number after judging all adjacent discrete points. If the number is an even number, the loop is an inner loop, and vice versa, if the number is an odd number, it is an outer loop. Based on the periodic direction, the closed periodic surface can be divided into two cases: (1) closed surface with one periodic direction, such as U-periodic surface or V-periodic surface; (2) closed surface with two periodic directions, such as UV-periodic surface.

3.1 U or V direction periodic surface

The V-periodic surface is similar to the U-periodic surface. They both own one periodic direction. Thus, this paper only analyzes the U-periodic surface. The side surface of the cylinder is taken as an example and shown in Figure 6. There are four loops on the surface, namely L_0, L_1, L_2, L_3. The outer loop is the outer boundary curve of a closed periodic surface. They may not be the longest loop in three-dimensional space, but it must span the whole periodic surface and be unclosed in parameter space. For example, the parameter coordinate u of the points on the outer loop of the cylindrical face are distributed over the entire U-direction period. In other words, the outer loop must cross the periodic line, and if it crosses the periodic line many times, the number of times must be an odd number. The inner loop is a closed loop inside the closed periodic surface, and the two adjacent points on the loop do not cross the whole periodic surface in the parameter space. Since the inner loop is a closed loop inside the surface, if the inner loop intersects with the periodic line, the number of times across the periodic line is even. For example, the inner loop of the cylindrical face, signed by L_2 and L_3, the number of the intersections is 0 and 2 respectively.

3.2 UV direction periodic surface

For a UV-periodic surface, if the number that the boundary loop of the surface crosses the periodic curves in U or V direction is an odd number, then the loop is an outer loop, otherwise the loop is an inner loop. As shown in the above Figure 7, the largest outer surface of the geometric model is the UV-periodic surface. The periodic surface includes four loops, namely L_0, L_1, L_2, L_3 (see Figure 7a). The u-direction periodic curve and the v-direction periodic curve are L_{p0} and L_{p1} respectively, as shown in Figure 7b. The simple schematic diagram of the UV-periodic surface in the parameter space is shown in Figure 7c.

From Figure 7b and c, it can be seen that the loop L_0 crosses the u-direction periodic curve L_{p0} twice. There are two intersections between the loop and the periodic curve, and thus it is an inner loop. As shown in Figure 7c, intersections are dark blue points and red points respectively. An intersection point is represented as one color. For the loop L_1 which crosses u-direction periodic curve L_{p0} twice and v-direction periodic curve L_{p1} twice, it is also an inner

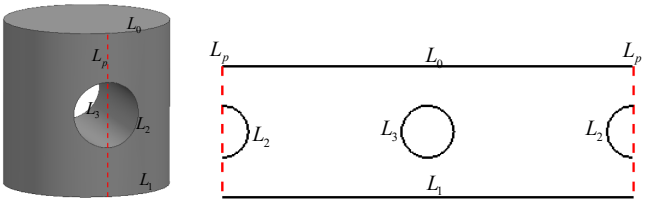

Figure 6.
U-periodic surface: (a) periodic surface of cylinder in physical space; (b) periodic surface of cylinder in parametric space

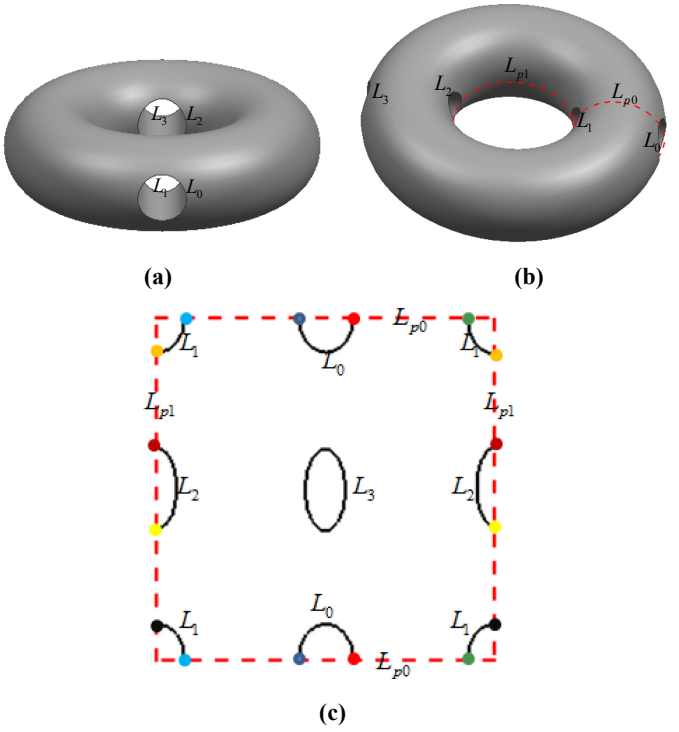

Figure 7.
UV-periodic surface: (a) toroidal solid; (b) periodic curves on the surface of toroidal solid; (c) periodic surface of toroidal solid in parametric space

loop. For the loop L_2 which crosses v-direction periodic curve L_{p1} twice, it is an inner loop. The loop L_3 does not cross u-direction periodic curve L_{p0} and v-direction periodic curve L_{p1}. The number that the loop L_3 crosses the periodic curves is zero, and thus the loop L_3 is the inner loop.

4. Results and comparisons

In this section, results for the algorithm proposed in this paper are shown to illustrate its accuracy and effectiveness. According to whether the surface is closed or not, this algorithm performs two sub-algorithms (APNM and CPNM, respectively). For non-closed surface (non-periodic surface and non-closed periodic surface), the APNM is employed. The effectiveness of APNM is illustrated by comparing with the ASM. The CPU time consumed by APNM and ASM is counted on an AMD Ryzen 5 processor 3.0 GHz. For a closed periodic surface, the CPNM is applied to determine the type of the loops, and the CPU time consumed by it is also counted.

4.1 Results for the APNM

The examples include planer surface and unclosed curved surface in this section. For the unclosed curved surfaces, the surfaces are unclosed in the three-dimensional physical space. However, in the parameter space, they are simply connected or multi connected region as the ordinary plane, or it can transfer to form a simply connected or multi connected region. Therefore, the judgment method is consistent with the ordinary plane and employs the APNM.

It can be seen from Figure 8–12 that the APNM, proposed in this article, has fewer segments than the ASM to discretize the boundary curves. Thus, the amount of calculation for the APNM is less than that of the ASM. In addition, the APNM only needs to judge the positive and negative of the area to judge the type of loops, while the ASM needs to compare the size of the

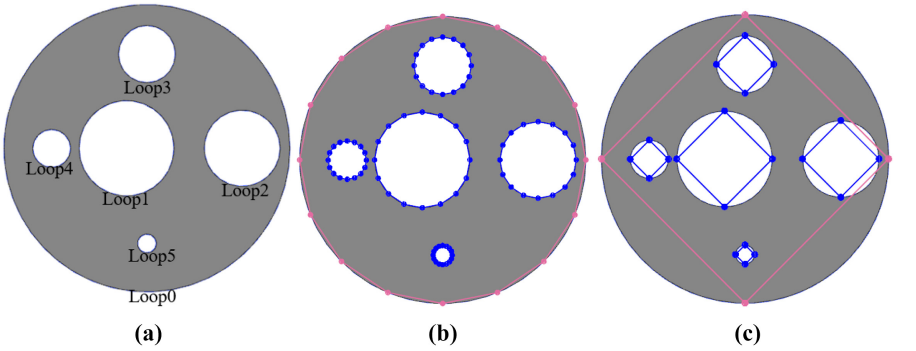

Figure 8.
Multi-loop plane:(a) loops on multi-loop plane; (b) discretized results of the ASM; (c) discretized results of the APNM

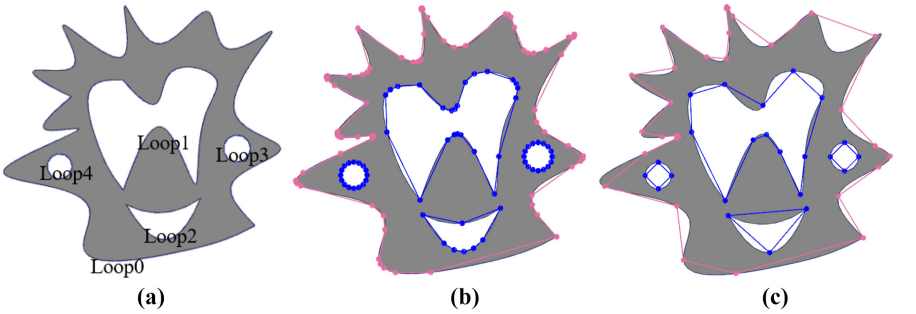

Figure 9.
Complex plane: (a) loops on complex plane; (b) discretized results of the ASM; (c) discretized results of the APNM

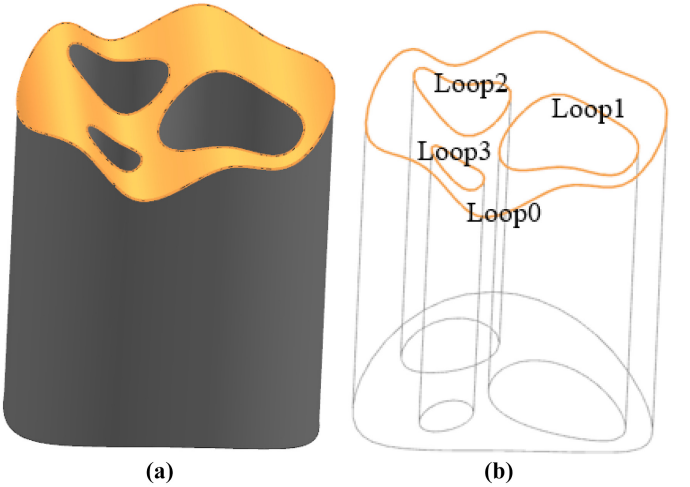

Figure 10.
Curved face on solid model: (a) solid model; (b) wire-frame model

area to judge the type of loops. Therefore, the calculation amount of the APNM is less than that of ASM. The area of loops on the surfaces is calculated and shown in Tables 1–3. In the APNM, the integral value of the polygon area is positive, the according loop is the outer loop. On the contrary, if the value is negative, the direction is clockwise, the according loop is an inner loop.

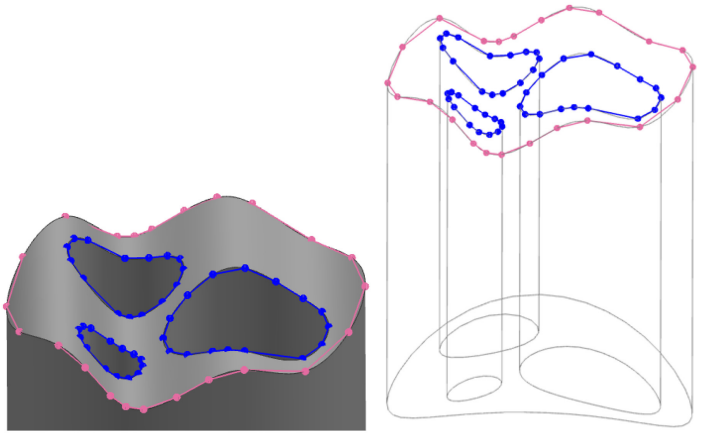

Figure 11.
Discretized results of curved surface for the ASM: (a) solid model; (b) wire-frame model

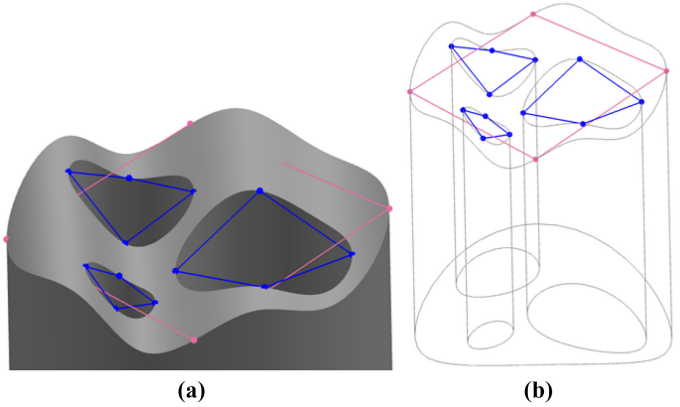

Figure 12.
Discretized results of curved surface for the APNM: (a) solid model; (b) wire-frame model

Method	Integral value of area					
	Loop0	Loop1	Loop3	Loop4	Loop5	Loop6
ASM	15,909.90	1767.77	1,131.37	636.40	282.84	70.71
APNM	11,250.00	−1,250.00	−800.00	−450.00	−200.00	−50.00

Table 1.
Area statistics of loops in multi-loop plane for two methods

Method	Integral value of area				
	Loop0	Loop1	Loop3	Loop4	Loop5
ASM	13,029.74	2,950.00	484.12	181.02	158.31
APNM	8,783.85	−2,116.22	−505.19	−128.00	−111.94

Table 2.
Area statistics of loops in complex plane for two methods

The inner loop judged by these two methods is marked blue discrete points, and the outer loop is marked by red discrete points. Since these two algorithms take very little time, in order to compare the efficiency of them, this article will run the two algorithms for one thousand times and then count the time. The time statistics are shown in Table 4. It is also illustrated from Table 4 that the efficiency of the APNM is higher than that of the ASM. Compared with the ASM, the more complex the model, the more time the APNM saves in the process of determining the inner and outer loops for non-closed surface.

In addition, after the inner and outer loops of a face are judged by APNM, meshing algorithm can discrete faces correctly. Meshing results generated by Advance Front Method (AFM) are shown in Figure 13.

Table 3.
Area statistics of loops in unclosed curved surface for two methods

Method	Integral value of area Loop0	Loop1	Loop3	Loop4
ASM	0.682	0.137	0.078	0.025
APNM	0.483	−0.097	−0.054	−0.017

Table 4.
Time statistics of two methods running 1,000 times

Method	Time (*ms*) Multi-loop plane	Complex plane	Curved surface
ASM	0.092	0.456	100.850
APNM	0.051	0.108	51.911

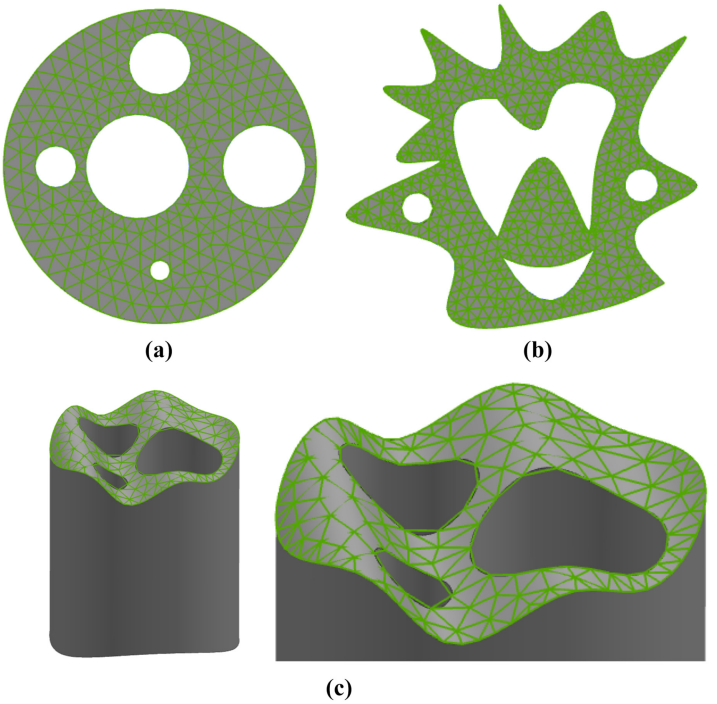

Figure 13.
Meshing results for faces: (a) multi-loop plane; (b) complex plane; (c) curved surface

4.2 Results for the CPNM

In this section, the closed U-periodic surface and UV-periodic surface are used as examples to illustrate the feasibility of the CPNM for judging the type of loops for the closed periodic surface.

Figure 14a is a perforated cylinder model, and the periodic surface of the perforated cylinder is highlighted in Figure 14b. This surface is the U-periodic surface, and the red dashed line is the periodic line of the periodic surface. It can be seen from Figure 14c and d that two loops are discrete by pink points, and both of them have two discrete points that cross the periodic line once, so they are both outer rings. And the four loops that are discrete by blue discrete points, of which one loop crosses the period line twice and the other three loops do not cross the period line, so these loops are all inner loops.

Figure 15a is the toroidal solid model after longitudinal sectioning, the highlight in Figure 15b is the UV-periodic surface, and the red dashed line is the periodic curve in two periodic directions. It can be seen from Figure 15c and d that there are two loops that are discretized as pink discrete points, and they respectively have two discrete points that cross the periodic curve once, so they are both outer loops. Among the two loops discretized as blue points, one loop crosses the period curve twice, and the other loop does not cross the period curve, so these loops are inner loops. In addition, after the inner and outer loops of a face are judged by CPNM, meshing algorithm can discrete faces correctly. Meshing results generated by Advance Front Method (AFM) are shown in Figure 16.

Since the ASM cannot judge the loop-type of a closed periodic surface, the CPNM cannot be compared with ASM. To demonstrate the efficiency of the CPNM, the CPNM in this study runs for one thousand times and the time statistics are given in Table 5. It is worth noting that the single run-time of CPNM is very small and can reach the level of microseconds.

The APNM and CPNM had been integrated in a CAE simulation software developed by our team (Center for Complete Solid Analysis). Figure 17 shows a Dirichlet problem on a trimmed torus calculated by the software. Figure 18 shows simulation results for steady-state heat conduction problem of the water cup calculated by the software. Their specific details can be found in reference (Zhang *et al.*, 2019, 2021).

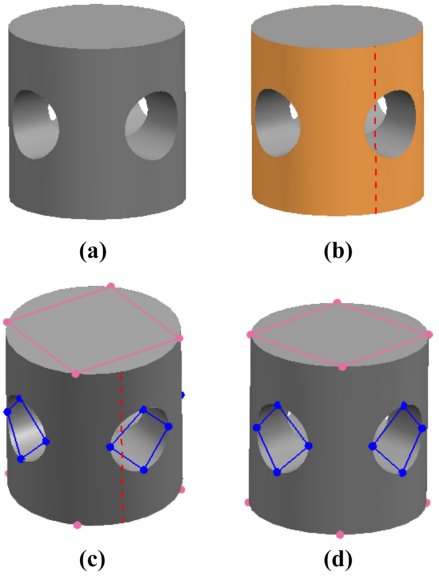

Figure 14.
Periodic surface of perforated cylinder: (a) perforated cylinder; (b) periodic surface and periodic line; (c) front view of the boundary curve after discretization; (d) rear view of the boundary curve after discretization

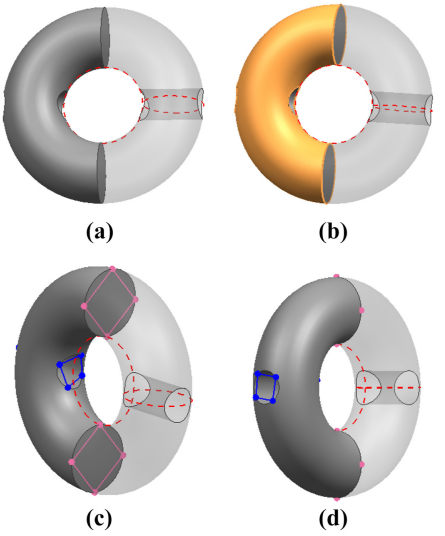

Figure 15.
Periodic surface of toroidal solid: (a) toroidal solid after slitting; (b) periodic surface and periodic curve; (c) front view of the boundary curve after discretization; (d) rear view of the boundary curve after discretization

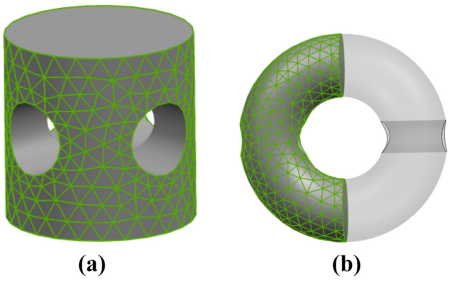

Figure 16.
Meshing results for closed periodic surfaces: (a) perforated cylinder; (b) toroidal solid

Table 5.
Time statistics of CPNM running 1,000 times

Method	Time (*ms*)	
	Periodic surface of perforated cylinder	Periodic surface of toroidal solid
CPNM	3.360	4.171

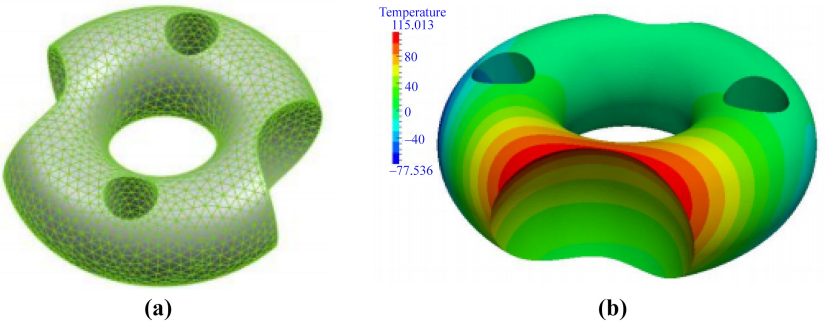

Figure 17.
Dirichlet problem on a trimmed torus (Zhang *et al.*, 2019): (a) mesh generation of the trimmed torus; (b) the contour plots of temperature in the whole domain

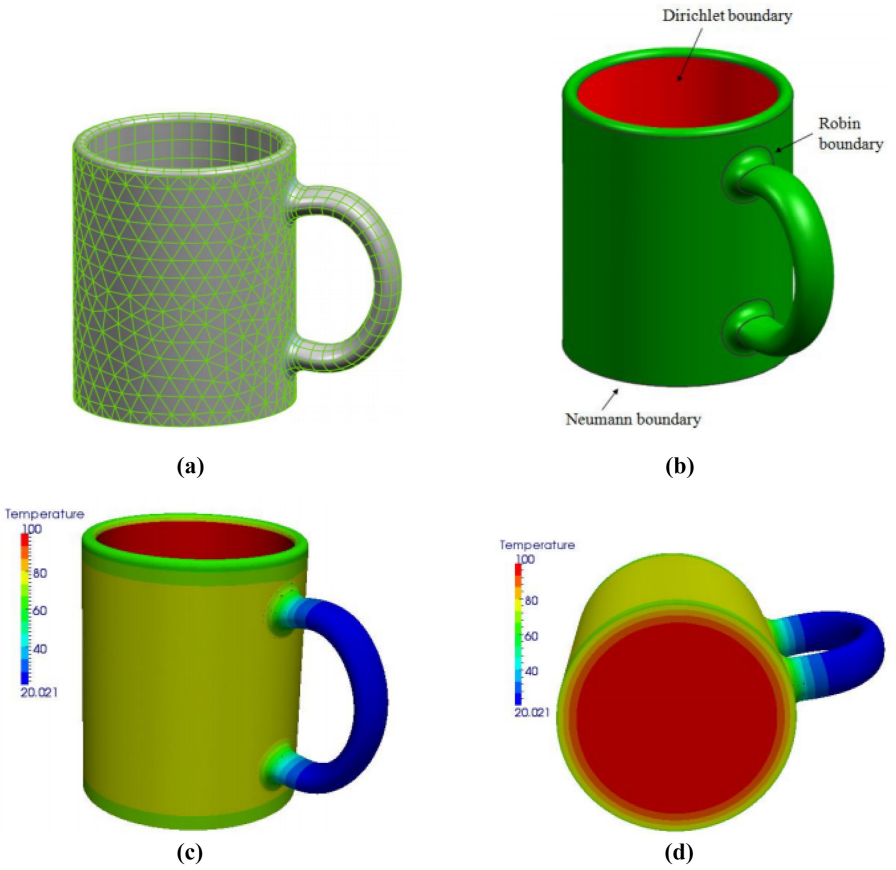

Figure 18. Simulation process for steady-state heat conduction problem of the water cup (Zhang *et al.*, 2019): (a) meshing generation of the cup; (b) boundary conditions of the cup; (c) temperature distribution in main view; (d) temperature distribution on the bottom face outside the cup

5. Conclusion

The algorithm proposed in this paper realizes the judgment of loop-type for an arbitrary parametric surface. According to whether the surface is closed or not, this algorithm considers two sub-algorithms (APNM and CPNM, respectively). For a non-closed surfaces, the first sub-algorithm (APNM) employs the dichotomy method to discretize the objective loop on the non-closed surfaces and then obtains the polygon in the parameter space of the surface. By combining the basic algorithm of polygon, the APNM can effectively determine the type of loop. For closed surfaces, the second sub-algorithm (CPNM) combines the dichotomy method with the periodicity of the closed surface to judge the loop-type of the surface. Numerical examples illustrate that the algorithms proposed in this paper can accurately and efficiently determine the inner and outer loops for an arbitrary parametric surface and can be applied to mesh generation in subsequent simulation.

References

Ameddah, H. and Assas, M. (2011), "Bio-CAD reverse engineering of free-form surfaces by planar contours", *Computer-Aided Design and Applications*, Vol. 8 No. 1, pp. 37-42.

Center for Complete Solid Analysis software for Engineering Structures, available at: http://www.5acae.com/EnglishVersion/index.html.

Chen, H., Sheng, W., Xi, N., Song, M. and Chen, Y. (2015), "CAD-based automated robot trajectory planning for spray painting of free-form surfaces", *Industrial Robot*, Vol. 29 No. 5, pp. 426-433.

Du, G., Liu, S. and Huang, X. (2007), "Boundary pre-adjustment method for finite element mesh generation on closed surfaces", *Journal of South China University of Technology (Natural Science Edition)*, Vol. 35 No. 2, pp. 27-32.

Feito, F. and Torres, J.C. (1997), "Inclusion test for general polyhedral", *Computer S& Graphics*, Vol. 21 No. 1, pp. 23-30.

Feito, F., Torres, J.C. and Urena, A. (1995), "Orientation, simplicity, and in-clusion test for planar polygons", *Computers & Graphics*, Vol. 19 No. 4, pp. 595-600.

George, P.L. (1996), "Automatic mesh generation and finite element computation", *Handbook of Numerical Analysis*, Vol. 4 No. 96, pp. 69-190.

Guan, Z., Sui, X., Gu, Y. and Li, Y. (2003a), "Automatic finite element mesh generation over 3D combined surfaces", *Chinese Journal of Computational Mechanics*, Vol. 20 No. 4, pp. 409-416.

Guan, Z., Song, C., Gu, Y. and Sui, X. (2003b), "Recent advances of research on finite element mesh generation methods", *Journal of Computer-Aided Design and Computer Graphics*, Vol. 15 No. 1, pp. 1-14.

Hoffmann, C.M. (1989), *Geometric and Solid Modeling*, CA Press, San Mateo, pp. 36-45.

Ke, Y. (2005), *Modeling Theory, Method and System of Reverse Engineering CAD*, Science Press. Machinery Industry Press, Beijing.

Li, S., Liu, H. and Fang, H. (2011), *Multivariate Calculus of Advanced Mathematics [M]*, Science Press, Beijing.

Lo, S.H. (2015), *Finite Element Mesh Generation*, CRC Press, New York, pp. 16-18.

Nasri, A.H. (1987), "Polyhedral subdivision methods for free-form surfaces", *Acm Transactions on Graphics*, Vol. 6 No. 1, pp. 29-73.

Shewchuk, J.R. (2014), "Delaunay refinement algorithms for triangular mesh generation", *Computational Geometry Theory and Applications*, Vol. 47 Nos 1-3, pp. 741-778.

Shi, L. and Xiao, X. (1997), "Direction of contour-loop and determination of inner and outer contour-loop", *Computer Engineering and Applications*, Vol. 033 No. 011, pp. 36-37.

Tate, S.J. and Jared, G.E.M. (2003), "Recognizing symmetry in solid models", *Computer-Aided Design*, Vol. 35 No. 7, pp. 673-692.

Thompson, J.F., Soni, B.K. and Weatherill, N.P. (1999), *Handbook of Grid Generation*, CRC Press, New York, pp. 525-528.

Wolfe, R. (2002), "Teaching visual aspects in an introductory computer graphics course", *Computers & Graphics*, Vol. 26 No. 1, pp. 163-168.

Zhang, J., Chi, B., Lin, W. and Ju, C. (2019), "A dual interpolation boundary face method for three-dimensional potential problems", *International Journal of Heat and Mass Transfer*, Vol. 140, pp. 862-876.

Zhang, J., Ju, C., Wen, P., Shu, X., Lin, W. and Chi, B. (2021), "A dual interpolation boundary face method for 3D elasticity", *Engineering Analysis with Boundary Elements*, Vol. 122, pp. 102-116.

Zheng, Y. and Chen, J. (2016), *Unstructured Mesh Generation: Theries, Algorithms and Applications*, Science Press, Beijing, pp. 19-20.

Zlatko, G. (1998), "A study on computer-based geometric modelling in engineering graphics", *Computer Networks*, Vol. 30 Nos 20/21, pp. 1915-1922.

Corresponding author
Chuanming Ju can be contacted at: cmju@hnu.edu.cn